ISSN 1819-7140, Russian Journal of Pacific Geology, 2007, Vol. 1, No. 1, pp. 82–97. © Pleiades Publishing, Ltd., 2007.
Original Russian Text © I.A. Tararin, V.M. Chubarov, E. K. Ignat'ev, S.V. Moskaleva, 2007, published in Tikhookeanskaya Geologiya, 2007, Vol. 1, No. 1, pp. 94–110.

Geology, Mineralogy, and PGE Mineralization of the Copper–Nickel Occurrences of the Kvinum Ore Field, Sredinny Range, Kamchatka

I. A. Tararin[a], V. M. Chubarov[b], E. K. Ignat'ev[c], and S. V. Moskaleva[b]

[a] *Far East Geological Institute, Far East Division, Russian Academy of Sciences, Vladivostok, Russia*
[b] *Institute of Volcanology and Seismology, Far East Division, Russian Academy of Sciences, Vladivostok, Russia*
[c] *Amur Minerals Corporation, Vladivostok, Russia*

Received June 6, 2006

Abstract—The geology and mineralogy of host metamorphic rocks, the mineralogy of sulfide ores, and the distribution of PGE mineralization were studied in detail for the Kvinum-1 and Kvinum-2 copper–nickel occurrences of the Kvinum ore field, which are the most promising targets for the copper–nickel–PGE mineralization of the Sredinny Range of Kamchatka. It was established that stringer–disseminated and massive copper–nickel ores are localized in amphibole peridotites, cortlandites, and form ore bodies varying from tens of centimeters to 5–20 m thick among the layered cortlandite–gabbroid massifs. The massive sulfide ores were found only at the bottom of cortlandite bodies and upsection grade into stringer–disseminated and disseminated ores. Pyrrhotite, chalcopyrite, and pentlandite are the major ore minerals with a sharply subordinate amount of pyrite, sphalerite, galena, arsenopyrite, and löllingite. Besides pentlandite, the Ni-bearing minerals include sulfoarsenides (gersdorffite), arsenides (nickeline), and tellurides (melonite) of nickel. It was found that PGE mineralization represented by antimonides (sudburyite) and tellurobismuthides (michenerite) of Pd with sharply subordinate platinum arsenide (sperrylite) is confined to the apical parts of massive sulfide zones and the transition zone to the stringer–disseminated ores. Ore intervals enriched in arsenides and tellurides of Ni, Pd, and Bi contain high-purity gold. In the central parts of the orebodies, the contents of PGE and native gold are insignificant. It is suggested that the contents of major sulfide minerals and the productivity of PGE mineralization in the cortlandites are defined by combined differentiation and sulfurization of ultramafic derivatives under the effect of fluids, which are accumulated at the crystallization front and cause layering of parental magmas with different sulfur contents. The fluid-assisted layering of mafic–ultramafic massifs resulted in the contrasting distribution of PGM in response to uneven distribution of sulfur (as well as As, Te, and Bi) during liquid immiscibility. The productivity of PGE mineralization significantly increases with increasing contents of S, As, Te, and Bi (elements to which Pt and, especially, Pd have high affinity) in fluids.

Key words: *copper–nickel–PGE mineralization, occurrences, cortlandites, metamorphic rocks, Late Cretaceous, Sredinny Range, Kamchatka.*

DOI: 10.1134/S1819714007010095

INTRODUCTION

The east coast of Asia contains widespread sulfide deposits and Cu–Ni occurrences related to specific Ca–Al-undersaturated amphibole peridotites—cortlandites [4, 21]. They contain abundant bodies of high-grade copper–nickel ore, which are comparable in size to the cortlandite massifs. The ore-bearing massifs are the swarms of small dikes and sills, which often show mafic–ultramafic layering and intense metasomatic amphibolitization. Cortlandite-related deposits and occurrences were found in North Korea, China, the Philippines, and Primorye. Detailed geological studies showed that Kamchatka is one of the promising Ni-bearing provinces in Russia [16, 17, 21, 24].

Numerous small mafic–ultramafic bodies of gabbro–cortlandite [22] or peridotite–pyroxenite–norite [16] associations with sulfide occurrences of complex PGE-bearing copper–nickel ores were found in the Sredinny Range of Kamchatka. Sulfide copper–nickel occurrences of the Sredinny Range form several ore fields: Shanuch, Dukuk, Kuvalorog, and Kvinum. The Shanuch and Kvinum ore fields are the most promising for economic PGE-bearing Cu–Ni mineralization [3, 16, 20, 21, 24].

The Kvinum ore field (~100 km^2 in area) is situated in the southern Sredinny Range on the left bank of the Kvinum River [3, 5, 16, 20, 24]. About 20 small cortlandite–gabbro massifs from a few to 200 m thick were mapped there. Five massifs contain sulfide copper–nickel mineralization. These are the Kvinum-1, Kvi-

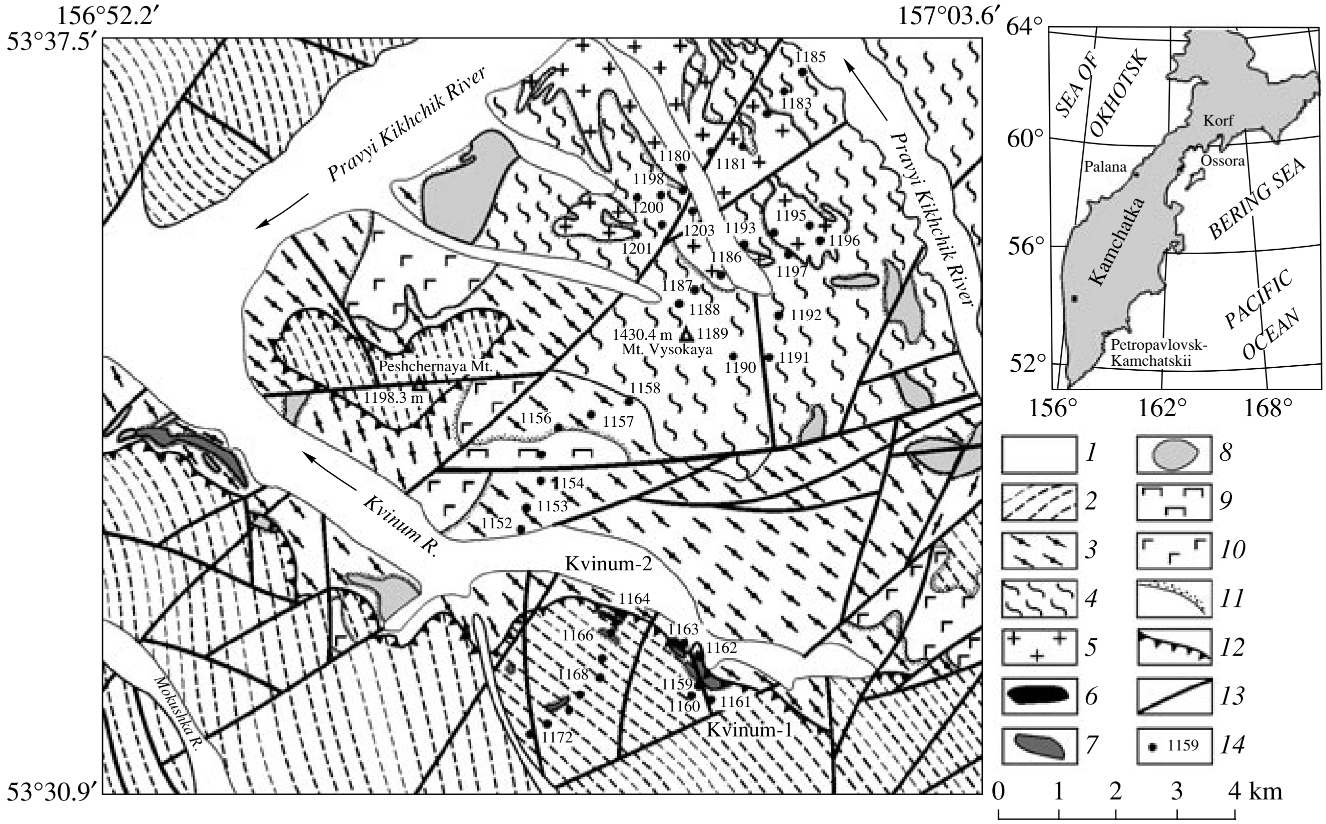

Fig. 1. Schematic geological map of the Kvinum ore field, southern Sredinny Range (modified after the materials of V.I. Sidorenko). The inset shows the position of the Kvinum ore field (filled box)

(*1*) Quaternary alluvial–talus deposits; (*2–4*) Upper Mesozoic metamorphic rocks (from top to bottom): (*2*) Kheivan Formation: garnet–mica ± andalusite schists, phyllites, and micaceous metasandstones; (*3*) Kamchatka Group (Shikhta Formation): andalusite–garnet–mica schists with rare intercalations of amphibole schists; (*4*) Kolpakov Group: kyanite–garnet–mica plagiogneisses and schists, migmatized plagiogneisses, migmatites, amphibolites, and garnet amphibolites; (*5–10*) intrusive rocks: (*5*) Krutogorskii Complex (?): gneissic tonalites, granodiorites, and rare trondhjemites; (*6, 7*) Dukuk Complex: (*6*) cortlandite, hornblendite, (*7*) gabbro, gabbronorite, gabbrodiorite; (*8*) Kola Complex: granodiorite, tonalite, plagiogranite, and trondhjemite; (*9, 10*) Alistor Complex: (*9*) metapicrites, (*10*) metadolerites, metabasalts, (*11*) contact hornfels, (*12*) overthrust, (*13*) faults, (*14*) observation points.

num-2, Tundrovoe, Kortlanditovoe, and Yasnoe occurrences. In this work, we summarized new geological and mineralogical data on the Kvinum-1 and Kvinum-2 occurrences and described zoning of the associated PGE mineralization (Fig. 1).

GEOLOGY OF THE COPPER–NICKEL OCCURRENCES

The cortlandite–gabbroid intrusions pertain to the Late Cretaceous Dukuk intrusive complex. They are correlated with the Andrianov Formation of the Sredinny Range and cut across the Late Mesozoic organic-rich metaterrigenous rocks of the Kolpakov and Kamchatka groups and the Kheivan Formation of the Malkin Group [5, 18]. The abundance of organic-rich xenoliths resulted in the wide development of graphite and the low oxidation state of rock-forming minerals.

The rocks of the Kheivan Formation compose an upper part of the metamorphic sequence in the study area (Fig. 1) and consist of garnet–mica (± staurolite) and andalusite–garnet–mica schists, which upsection grade into phyllites and micaceous sandstones (Fig. 2), thus demonstrating a decrease in the metamorphic grade from amphibolite (T = 520–580°C, P = 1.4–3.3 kbar, Table 1) to green-schist facies biotite–muscovite and muscovite–chlorite subfacies. These rocks show thin foliation at a high angle (30°–40° and more) to their bedding. In the Kvinum River basin, the W–E-trending primary bedding of sedimentary rocks is overprinted by intense north-west-trending foliation. The angular discordance between the bedding and overprinted foliation resulted in the abundance of small folds, micro and macroboudinage, and numerous detachments that are especially typical of the metapsammitic rocks. The rocks of the Kheivan Formation contain numerous quartz veins, lenses, and segregations, which are concordant to foliation and, as the host rocks, are fragmented into individual lenses and blocks, thus attenuating the dislocations.

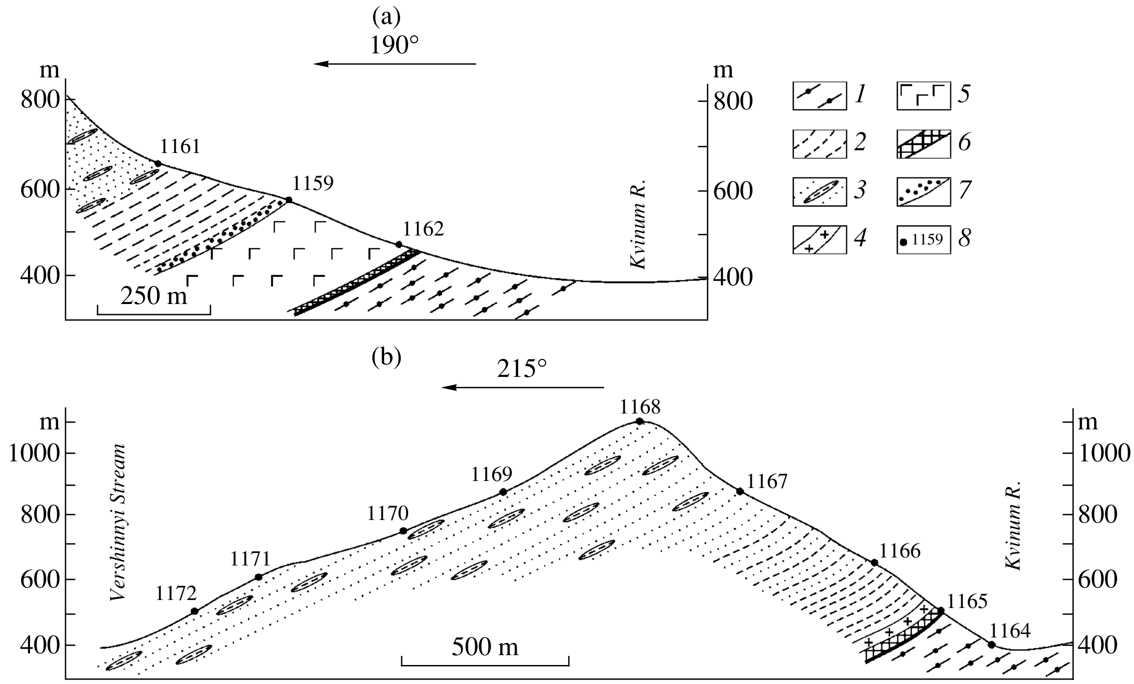

Fig. 2. Schematic geological section across the Kvinum-1 (a) and Kvinum-2 (b) occurrences of the Kvinum ore field.
(*1*) Kamchatka Group (Shikhta Formation): andalusite–garnet–mica schists; (*2, 3*) Kheivan Formation: garnet–mica ± andalusite schists, phyllites (*2*), micaceous metasandstones with phyllite intercalations (*3*); (*4*) Kola intrusive complex (?): schistose aplitic granites; (*5, 6*) Dukuk intrusive complex: gabbro, gabbronorite (*5*), cortlandite, and hornblendite (*6*); (*7*) contact hornfels, (*8*) observation points.

The deposits of the Kheivan Formation are overthrust at a low angle on the crystalline schists of the Kamchatka Group (the Shikhta Formation). Remains of this nappe occur on the right bank of the Kvinum River (Mt. Peshchernaya, Fig. 1) and as a 25-m-thick cap on Mt. Vysokaya (not shown in the geological scheme in Fig. 1).

Metasedimentary rocks of the Kamchatka Group include andalusite-bearing garnet–staurolite–mica schists of amphibolite facies ($T = 550°C$, $P_s = 3.3–4.5$ kbar, Table 1). Down-section, the rocks of the group are weakly migmatized and contain concordant or, more rarely, discordant synmetamorphic granite and pegmatite bodies.

In the Kvinum–Pravyi Kikhchik interfluve, the deposits of the Kamchatka Group are cut by metapicrites and metadolerites of the Alistor (?) intrusive complex, as well as by tonalites, granodiorites, and trondhjemites of the Kola Complex (Fig. 1).

The Kamchatka Group rests disconformably on the metamorphic rocks of the Kolpakov Group located at the base of the Sredinny Range metamorphic sequence. The Kolpakov Group is made up of migmatized kyanite–garnet–mica (occasionally with staurolite) plagiogneisses and migmatites, which contain bodies of mafic clinopyroxene–amphibole schists, amphibolites and garnet amphibolites up to 20–50 m thick, as well as numerous synmetamorphic granites and pegmatites. The Kolpakov deposits also contain large intrusions of gneissic granitoids (tonalites, granodiorites, and more rarely, trondhjemites) of the Krutogorskii complex.

In this area, the rocks of the Kolpakov Group are metamorphosed under the amphibolite-facies kyanite subfacies ($T = 530–590°C$, $P_s = 4.2–4.8$ kbar, Table 1), which defines the wide development of kyanite in aluminous assemblages of metamorphic rocks. Similar metamorphic parameters were determined by garnet–amphibole geothermometer [25] and experimental amphibole–plagioclase geobarometer [15] for Ca-rich mineral assemblages of the Kolpakov rocks (Table 1).

The comparison of the physicochemical metamorphic parameters of the Kheivan Formation and Kamchatka and Kolpakov groups (Table 1) indicates a gradual down-section increase in the metamorphic grade pressure (depth) from the andalusite to kyanite assemblages across the metamorphic sequence of the Sredinny Range.

The protoliths of crystalline schists, phyllites, and micaceous metasandstones of the Kheivan Formation (Table 2) are diverse sedimentary rocks: from montmorillonite clays to dolomitic sandstones and graywackes, with predominant Na–Mg montmorillonite clays of moderate to high Fe and high Al contents [12].

The Kamchatka Group (the Shikhta Formation) is dominated by aluminous garnet–mica and andalusite–garnet–mica (± staurolite) schists (Table 2). They were

Table 1. Composition of the minerals (wt %) and the metamorphic temperature and pressure of the rocks of the Kheivan, Shikhta, and Kolpakov groups of the Kvinum ore field

Sample	Mineral	SiO_2	TiO_2	Al_2O_3	FeO	MnO	MgO	CaO	Na_2O	K_2O	Total	X_{Mg}	T, °C	$P_s \times 10^8$ Pa	Assemblage
1	2	3	4	5	6	7	8	9	10	11	12	13	14	15	16
Kheivan Formation															
1162/10	Gr_c	37.37	0.00	21.78	31.91	6.14	2.19	1.25	0.00	0.00	100.64	0.093	561[1]	1.4[8]	Gr + Sta + Bi + Pl + Q
	Gr_r	36.85	0.00	21.63	32.41	6.08	2.19	0.99	0.00	0.00	100.15	0.092			
	Bi	34.70	1.46	20.99	19.60	0.13	7.97	0.00	0.28	9.16	94.29	0.419			
	Pl_r	62.70	0.00	35.35	0.13	0.00	0.00	4.60	9.08	0.11	99.97	0.217[9]			
1165/6	Gr_c	36.44	0.00	21.64	36.85	1.76	2.94	0.90	0.00	0.00	100.53	0.119	520[1]	2.4[7]	Gr + Bi + Mu + Pl + Or + Q
	Gr_r	36.83	0.00	21.46	35.22	3.18	2.07	1.06	0.00	0.00	99.82	0.088			
	Bi	34.70	1.16	21.21	21.11	0.04	9.13	0.00	0.31	8.85	96.51	0.435			
	Mu	43.75	0.28	36.82	0.84	0.00	0.47	0.00	1.17	9.11	92.44	0.500			
	Pl_r	63.32	0.00	22.95	0.58	0.00	0.00	4.26	9.28	0.12	100.51	0.201[9]			
1204/2	Gr_c	37.11	0.00	21.59	32.72	5.08	2.08	1.72	0.00	0.00	100.30	0.089	547[1]	1.3[7]–2.4[8]	Andl + Gr + Cor + Sta + Bi + Mu + Pl + Q
	Gr_r	37.18	0.00	21.76	35.52	3.58	2.09	1.07	0.00	0.00	101.20	0.087			
	Bi	34.14	1.47	20.69	21.19	0.06	7.99	0.00	0.35	9.05	94.94	0.401			
	Mu	46.99	0.21	36.06	0.97	0.00	0.74	0.00	0.71	8.50	94.18	0.577			
	Cor	47.99	0.00	33.66	9.86	0.15	6.88	0.00	0.06	0.00	98.60	0.551			
	Pl_r	62.85	0.00	23.62	0.32	0.00	0.00	4.84	8.97	0.12	100.72	0.228[9]			
1159	Gr_c	37.58	0.00	21.83	31.40	1.24	5.68	2.17	0.00	0.00	99.90	0.237	587[1]	3.3[8]	Andl + Gr + Bi + Mu + Pl + Q + Ilm
	Gr_r	37.68	0.00	21.69	34.82	1.36	3.14	2.06	0.00	0.00	100.75	0.134			
	Bi	35.88	1.00	21.50	20.02	0.05	9.28	0.00	0.05	9.30	97.08	0.452			
	Mu	45.37	0.30	36.56	1.40	0.00	0.45	0.00	0.51	8.41	93.00	0.365			
	Pl_r	59.03	0.00	26.18	0.98	0.00	0.00	7.48	7.35	0.08	101.10	0.358[9]			
Kamchatka Group (Shikhta Formation)															
1153/1	Gr_c	37.19	0.00	22.00	31.60	4.23	0.97	4.92	0.00	0.00	100.91	0.046	550[1]	4.5[8]	Andl + Gr + Sta + Bi + Mu + Pl + Q + Ilm
	Gr_r	37.02	0.00	22.01	36.43	1.14	1.92	2.70	0.00	0.00	101.22	0.083			
	Sta_r	26.61	0.46	57.40	13.28	0.03	0.89	0.01	0.05	0.00	99.12*				
	Bi	34.58	1.23	21.25	22.25	0.03	7.21	0.00	0.06	9.49	96.10	0.366			
	Mu	46.36	0.26	36.72	1.38	0.00	0.52	0.00	0.64	9.29	95.17	0.402			
	Pl_r	61.35	0.00	24.45	0.33	0.00	0.00	5.87	8.47	0.23	100.70	0.273[9]			

Table 1. (Contd.)

1	2	3	4	5	6	7	8	9	10	11	12	13	14	15	16
1204/1	Gr_c	37.27	0.00	21.64	33.24	4.06	1.98	2.43	0.00	0.00	100.62	0.086	549[1)]	3.3[8)]–4.1[7)]	Andl + Gr + Sta + Bi + Mu + Pl + Ilm
	Gr_r	37.09	0.00	21.57	35.03	3.45	2.06	2.03	0.00	0.00	101.23	0.087			
	Sta_r	27.37	0.38	57.15	13.59	0.17	1.15	0.00	0.00	0.00	99.95*	0.129			
	Bi	34.65	1.49	20.66	21.35	0.08	7.95	0.00	0.22	9.10	95.50	0.398			
	Mu	50.39	0.17	35.30	1.20	0.00	1.17	0.00	0.50	8.79	97.52	0.635			
	Pl_r	61.93	0.00	24.34	0.05	0.00	0.00	5.77	8.41	0.09	100.59	0.274[9)]			
Kolpakov Group															
1180/3	Gr_c	37.22	0.00	21.85	36.97	2.06	2.46	1.03	0.00	0.00	101.58	0.101	577[1)]	4.5[7)]	Gr + Sta + Bi + Mu + Pl + Q
	Gr_r	37.30	0.00	21.77	35.19	3.41	2.04	1.34	0.00	0.00	101.05	0.086			
	Sta_r	26.79	0.48	57.24	13.52	0.17	1.26	0.00	0.01	0.00	100.13*3	0.142			
	Bi	34.31	2.15	20.98	21.39	0.03	6.74	0.00	0.06	8.69	94.35	0.359			
	Mu	45.64	0.88	36.28	0.83	0.01	0.46	0.00	0.58	8.99	93.57	0.494			
	Pl_r	64.28	0.00	22.32	0.49	0.00	0.00	3.43	9.79	0.08	100.39	0.162[9)]			
1195	Gr_c	37.46	0.00	21.57	32.23	6.73	1.73	0.90	0.00	0.00	100.62	0.073	581[1)]	–	Gr + Bi + Pl + Or + Q
	Gr_r	37.02	0.00	21.68	31.86	8.26	1.22	0.87	0.00	0.00	100.91	0.051			
	Bi	34.13	2.37	20.29	24.00	0.32	4.99	0.00	0.01	9.81	95.85	0.268			
	Pl_r	63.68	0.00	23.25	0.46	0.00	0.00	3.88	9.96	0.23	101.46	0.175[9)]			
1201/1	Gr_c	37.14	0.00	21.86	35.14	2.62	2.69	1.71	0.00	0.00	101.16	0.113	586[1)]	4.8[8)]	Ky + Gr + Sta + Bi + Mu + Pl + Q
	Gr_r	37.11	0.00	21.83	34.46	3.45	2.14	2.09	0.00	0.00	101.08	0.091			
	Sta_r	26.61	0.56	57.24	13.55	0.21	1.86	0.00	0.01	0.00	99.44*4	0.131			
	Bi	34.69	1.82	21.15	22.14	0.65	7.29	0.00	0.06	9.10	96.90	0.363			
	Pl_r	62.81	0.00	23.49	0.31	0.00	0.00	4.93	8.97	0.09	100.60	0.232[9)]			
1184/3	Bi^1	35.40	2.69	19.32	18.90	0.14	9.19	0.01	0.06	9.89	95.60	0.462	530[2)]	–	Mu + Bi + Pl + Q
	Bi^2	34.13	2.30	20.29	24.00	0.32	4.99	0.00	0.01	9.81	95.85	0.268			
	Mu	45.80	0.83	35.43	0.95	0.05	0.77	0.00	0.41	10.03	94.27	0.579			
	Pl_r	64.05	0.00	22.85	0.06	0.00	0.00	3.73	9.56	0.36	100.61	0.174[9)]			

Table 1. (Contd.)

1	2	3	4	5	6	7	8	9	10	11	12	13	14	15	16
1192/4	Gr_c	37.69	0.00	21.73	20.98	11.31	0.48	7.90	0.00	0.00	100.09	0.026	560[5)]	4.2[5)]	Gr + Hb + Pl ± Or + Ilm
	Gr_r	37.80	0.00	21.58	25.91	4.80	1.27	9.23	0.00	0.00	100.59	0.067			
	Hb_r	44.64	0.74	11.14	20.87	0.27	7.83	10.86	1.60	0.40	98.35	0.398			
	Pl_c	61.14	0.00	24.38	0.19	0.00	0.00	5.96	8.41	0.17	100.25	0.279[9)]			
	Pl_r	59.08	0.00	26.28	0.43	0.00	0.00	7.49	7.38	0.05	100.71	0.358[9)]			
1195/4	Gr_c	37.13	0.00	21.22	29.13	2.59	1.45	8.76	0.00	0.00	100.28	0.075	560[6)]	4.5[7)]	Gr + Hb + Cum + Pl + Ilm
	Gr_r	37.18	0.00	21.12	31.49	1.53	1.86	7.95	0.00	0.00	101.13	0.091			
	Hb_c	45.55	0.94	10.59	22.29	0.27	7.60	10.24	1.89	0.25	99.62	0.375			
	Hb_r	44.60	0.54	10.86	21.72	0.20	6.28	10.78	1.36	0.36	96.70	0.338			
	Cum	52.32	0.03	0.88	32.39	0.69	11.30	1.05	0.03	0.00	98.69	0.378			
	Pl_c	60.65	0.00	24.98	0.12	0.00	0.00	6.43	8.01	0.08	100.27	0.306[9)]			
	Pl_r	59.44	0.00	25.75	0.49	0.00	0.00	7.34	7.49	0.05	100.56	0.350[9)]			
1189	Cpx_c	52.01	0.03	0.92	10.94	0.26	10.85	23.31	0.04	0.00	98.39**	0.633	700[4)]	–	Cpx + Hb + Pl
	Hb_c	51.28	0.27	5.70	14.74	0.22	12.48	12.09	0.48	0.05	97.31	0.598			
	Hb_r	48.47	0.29	7.55	15.57	0.21	11.64	11.93	0.61	0.08	96.35	0.568			
	Pl_c	45.55	0.00	35.17	0.20	0.00	0.00	17.64	1.42	0.01	99.99	0.872[9)]			
	Pl_r	46.11	0.00	34.40	0.23	0.00	0.00	17.01	1.96	0.01	99.72	0.827[9)]			
1189/1	Hb_r	47.58	0.45	9.54	12.83	0.21	13.08	11.54	1.24	0.15	96.62	0.641	575[3)]	–	Hb + Pl
	Pl_r	54.92	0.00	28.85	0.38	0.00	0.00	10.93	5.32	0.07	100.47	0.529[9)]			

Note: Temperature: [1)] garnet–biotite [2, 5], [2)] biotite–muscovite [1], [3)] amphibole–plagioclase [15], [4)] clinopyroxene–plagioclase [14] equilibria, [5)] temperature and pressure on the basis of an experimental amphibole–plagioclase geothermobarometer [15], [6)] temperature on the basis of an amphibole–plagioclase geothermometer [25]. Pressure: [7)] after garnet–biotite–muscovite–plagioclase and [8)] after Gr–Pl–Al_2SiO_5 geobarometers [1]. [9)] Content of the anorthite end member in plagioclase X_{An} = Ca/(Ca + Na + K). X_{Mg} = Mg/(Mg + Mn + Fe). * Total additional includes ZnO (wt %): 1153/1—0.19, 1204/1—0.14, 1180/3—0.66, 1201/1—0.40. ** Total contains 0.03% Cr_2O_3. (1162/10) garnet–staurolite–biotite crystalline schist, (1165/6) garnet–mica schist, (1153/1, 1204/1, 1204/2, 1180/3) garnet–staurolite–mica (± andalusite) schist, (1159) andalusite–garnet–mica hornfels, (1195) garnet–biotite migmatite, (1201/1) migmatized garnet–staurolite–mica schist, 1184/3 micaceous migmatite, (1192/4, 1195/4) garnet amphibolites, (1189) clinopyroxene–amphibole mafic schist, (1189/1) melanocratic amphibolite. Position of samples is shown in Fig. 1. Hereinafter, the minerals were analyzed using a Camebax microprobe at the Institute of Volcanology and Seismology, Far East Division, Russian Academy of Sciences.

Table 2. Chemical composition of metamorphic rocks of the Kheivan Formation, Kamchatka and Kolpakov groups of the Kvinum ore field

Sample	1159	1159/7	1162/10	1165/6	1173/4	1175/1	1204/2	1166	1174	1153/1	1204/1
	1	2	3	4	5	6	7	8	9	10	11
SiO_2	55.25	63.50	68.20	64.00	64.00	66.70	63.00	74.10	66.40	54.10	63.30
TiO_2	1.25	0.74	0.69	0.82	0.92	0.74	0.92	0.38	0.62	1.08	0.90
Al_2O_3	20.28	18.95	15.58	15.82	17.28	15.14	15.64	11.00	15.51	23.00	15.27
Fe_2O_3	4.54	2.76	3.65	3.83	5.18	4.50	5.00	1.62	3.15	7.44	6.49
FeO	4.08	3.17	1.90	3.52	1.62	1.94	2.60	1.41	2.32	0.92	1.06
MnO	0.18	0.09	0.08	0.08	0.07	0.28	0.09	0.05	0.06	0.08	0.07
MgO	1.79	0.78	1.28	2.83	3.44	2.64	2.93	2.02	2.24	1.76	3.57
CaO	3.09	2.00	2.04	1.16	1.43	1.09	2.05	1.76	1.91	2.46	2.05
Na_2O	3.00	1.90	3.30	3.00	1.35	2.50	2.48	3.60	3.25	2.80	2.48
K_2O	1.56	2.56	2.00	2.61	2.55	2.61	2.50	2.40	2.15	3.40	2.35
P_2O_5	0.20	0.19	0.28	0.25	0.41	0.14	0.33	0.13	0.22	0.35	0.33
L.O.I.	4.51	3.00	1.09	2.06	1.56	1.59	2.31	1.50	2.00	2.60	2.12
Total	99.73	99.64	100.09	99.98	99.81	99.87	99.85	99.97	99.83	99.99	99.99
Rb	28	89	34	62	47	84	50	49	67	111	53
Sr	447	292	449	146	128	197	150	282	295	315	251
Ba	877	634	967	753	754	2357	706	662	569	628	611
Zr	226	242	208	168	193	140	197	165	114	260	214
Y	28	31	26	25	27	22	28	21	22	32	25
Nb	19	26	29	23	20	19	25	10	15	30	23
La	9	49	43	50	34	n.a.	34	25	32	50	33
Ce	28	80	24	43	54	8	52	45	31	88	53
Nd	n.a.	13	10	21	11	n.a.	13	3	3	27	12
Ni	48	88	65	119	98	75	59	56	57	58	91
Co	22	40	26	46	31	31	18	22	20	16	22
Cr	152	118	114	229	181	96	113	93	97	108	155
V	130	154	118	162	168	151	119	87	111	163	126
Cu	101	89	20	25	30	82	20	50	72	30	86

Sample	1180/3	1201/1	1180	1195	1199	1184/3	1192/4	1195/4	1180/1	1189
	12	13	14	15	16	17	18	19	20	21
SiO_2	66.30	66.50	73.80	64.50	68.90	72.50	49.40	50.00	49.50	52.20
TiO_2	0.76	0.90	0.53	0.65	0.68	0.62	2.26	2.91	0.77	1.07
Al_2O_3	15.80	14.50	12.35	16.60	13.60	13.05	17.12	10.65	15.37	16.90
Fe_2O_3	2.53	2.94	1.10	2.25	4.00	1.65	4.58	5.41	3.80	4.50
FeO	3.03	3.73	2.04	2.04	1.69	1.62	8.10	12.67	3.87	3.52
MnO	0.05	0.08	0.05	0.10	0.07	0.05	0.20	0.26	0.14	0.15
MgO	1.70	2.83	2.73	2.37	2.83	2.30	4.30	6.51	8.86	3.04
CaO	1.40	1.98	0.61	3.37	1.84	1.36	8.66	7.98	11.59	15.28
Na_2O	2.80	2.65	2.70	4.55	3.17	2.65	4.00	3.17	2.70	1.52
K_2O	2.75	2.05	2.83	1.95	1.94	2.05	0.20	0.07	0.10	0.10
P_2O_5	0.24	0.40	0.12	0.24	0.06	0.12	0.55	0.40	0.33	0.18
L.O.I.	2.60	1.33	1.10	0.94	1.00	2.00	0.61	–	2.93	1.37
Total	99.97	99.89	99.96	99.56	99.78	99.97	99.98	100.03	99.96	99.83
Rb	64	53	68	45	53	83	n.a.	4	n.a.	n.a.
Sr	228	251	255	224	248	225	331	216	139	157
Ba	836	611	1146	314	561	60.3	423	59	22	6
Zr	199	214	166	335	166	150	158	220	35	63
Y	26	25	16	45	22	23	37	45	18	24
Nb	27	23	22	28	24	20	5	9	0	63
La	20	33	20	55	24	31	n.a.	16	11	11
Ce	45	53	36	88	45	53	20	32	18	18
Nd	n.a.	12	n.a.	35	n.a.	n.a.	0	13	n.a.	3
Ni	56	71	107	13	70	19	114	39	158	70
Co	17	24	60	8	39	6	55	36	42	39
Cr	112	127	120	22	225	106	248	28	458	225
V	114	120	107	86	102	104	131	134	105	102
Cu	25	20	59	22	35	60	73	20		35

Table 2. (Contd.)

Sample	1189/1	1180/9	1181/1	1200	1165/4	1159/1	1178	1154/3	1155/5	1157/2
	22	23	24	25	26	27	28	29	30	31
SiO_2	51.10	73.10	71.10	72.10	76.00	53.50	54.20	44.30	43.55	43.85
TiO_2	1.11	0.53	0.66	0.53	0.18	0.46	0.69	0.08	0.38	0.26
Al_2O_3	14.16	13.48	13.80	10.00	11.66	17.40	14.10	3.76	9.95	8.56
Fe_2O_3	4.27	1.50	3.00	1.94	1.51	3.44	3.87	8.20	4.54	5.15
FeO	4.93	1.76	0.56	2.04	0.63	2.60	3.24	1.06	5.63	4.79
MnO	0.17	0.04	0.05	0.08	0.04	0.14	0.12	0.24	0.21	0.23
MgO	9.00	1.36	2.34	1.51	0.82	6.05	9.50	29.73	22.39	24.01
CaO	11.73	1.50	1.02	2.11	1.16	8.78	8.08	1.70	6.31	5.63
Na_2O	2.65	3.08	3.08	4.50	5.50	3.75	3.00	0.00	0.30	0.00
K_2O	0.04	2.15	2.72	3.65	1.72	1.55	0.50	0.00	0.00	0.00
P_2O_5	0.15	0.24	0.11	0.35	0.11	0.24	0.45	0.16	0.19	0.30
L.O.I.	0.70	1.15	1.43	1.08	0.65	2.00	1.95	10.19	6.03	7.00
Total	100.01	99.89	99.87	99.89	99.98	99.91	100.00	99.42	99.48	99.78
Rb	n.a.	54	110	101	20	n.a.	n.a.	n.a.	n.a.	n.a.
Sr	175	234	293	329	102	645	385	60	101	58
Ba	17	521	1244	749	479	251	246	n.a.	7	10
Zr	55	113	198	191	224	41	66	n.a.	n.a.	n.a.
Y	19	22	24	21	34	19	17	13	16	13
Nb	5	17	27	20	20	n.a.	7	n.a.	1	2
La	9	24	45	24	25	9	20	9	10	8
Ce	13	35	51	48	58	15	30	5	7	5
Nd	9	7	15	2	9	n.a.	n.a.	n.a.	n.a.	n.a.
Ni	85	27	39	38	8	268	105	548	383	463
Co	42	10	11	16	5	63	36	63	55	54
Cr	292	110	135	75	12	67	183	1194	863	729
V	97	101	120	109	27	79	106	42	84	71
Cu	101	45	20	40	15	124	66	20	40	72

Note: (1–9) Kheivan Formation: andalusite–garnet–mica hornfels; (2–7) garnet–mica ± staurolite ± andalusite ± cordierite schist; (8) biotite crystalline schist; (9) chlorite–sericite phyllite; (10, 11) Kamchatka Group (Shikhta Formation), andalusite–garnet–staurolite crystalline schist; (12–22) Kolpakov Group: (12–16) migmatized garnet–mica ± staurolite ± kyanite plagiogneisses, (17) muscovite–biotite plagiogneiss, (18, 19) garnet amphibolite, (20, 21) clinopyroxene–amphibole mafic schist, (22) amphibolite; (23–25) gneissic granitoids of the Krutogorskii (?) intrusive complex; (26) schistose biotite–muscovite aplitic granite of the Kola (?) intrusive complex; (27, 28) diaphthoritic gabbroids of the Dukuk intrusive complex; (29–31) Alistor (?) intrusive complex: metapicrites (29, 30), metadolerite (31). The major elements (wt %) were determined using the weight chemical method; the trace elements (g/t) were measured using the X-ray-radiometric and qualitative spectral methods.

formed after hydromica and montmorillonite clays, the rocks of Na–Mg series with high Fe and Al contents, which provided formation of garnet, staurolite, andalusite, high-Al biotite, and muscovite.

The Kolpakov Group is abundant in low-Ca (CaO ≤ 5 wt %) metaterrigenous rocks containing bodies of Ca-rich rocks (amphibolites, garnet amphibolites, and clinopyroxene–amphibole schists). The low-Ca rocks are dominated by garnet–mica (± staurolite, ± kyanite) plagiogneisses and their migmatized varieties, which were developed after montmorillonite and hydromica clays and, more rarely, graywackes [12]. All these rocks have high Al and Fe contents (Table 2).

The Ca-rich rocks of the Kolpakov Group in the study area are made up mainly of amphibolites and garnet amphibolites with moderate Fe and low Al contents (Table 2). It was shown that their protoliths were tholeiitic and calc–alkaline basalts and, to a lesser extent, basaltic andesites. The garnet amphibolites, as those over the entire metamorphic zone of the Sredinny Range, have a high Ti content (Table 2) and presumably

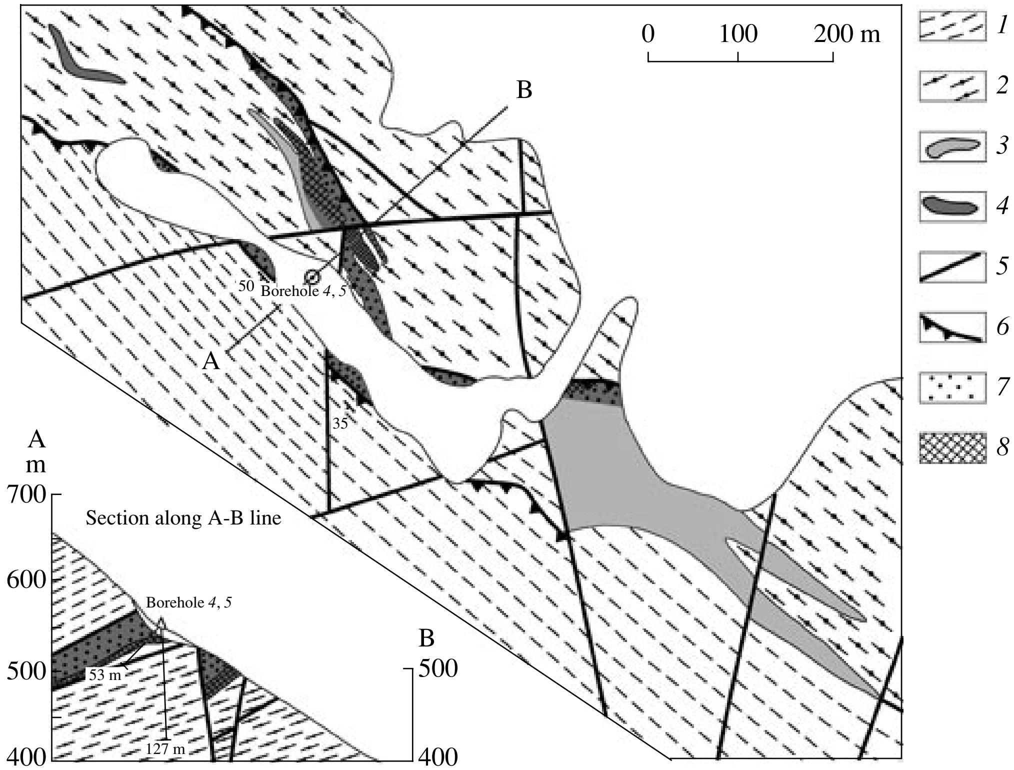

Fig. 3. Schematic geological plan and section along the A–B line of the Kvinum-1 occurrence.
(*1*) Kheivan formation: garnet–mica ± andalusite schists, phyllites, micaceous metasandstones; (*2*) Kamchatka Group (Shikhta Formation): andalusite–garnet–mica schists; (*3, 4*) Dukuk intrusive complex: gabbro, gabbronorites, gabbrodiorites (*3*), cortlandites, hornblendites (*4*); (*5, 6*) tectonic dislocations: faults (*5*), low-angle thrusts (*6*); (*7, 8*) copper–nickel ores: low-grade disseminated (*7*), high-grade massive and stringer–disseminated (*8*).

were formed by metamorphism of within-plate magmatic rocks.

KVINUM-I AND KVINUM-II OCCURRENCES

The Kvinum-I (Fig. 3) and Kvinum-II (Fig. 4) occurrences are situated in the central part of the Kvinum ore field, in the left-bank middle reaches of the Kvinum River. They are contained in small sill-like gabbro-cortlandite intrusions localized along the low-angle sublatitudinal thrust zone between the rocks of the Kheivan Formation and Kamchatka Group. The total extent of the massifs is about 1000 m at thicknesses from a few meters at the flanks of the intrusive bodies to 200 m in their central parts.

The intrusive bodies are bounded by zones of tectonic mélange, schistosity, and boudinage. The host rocks of the Kheivan Formation at the contacts were converted in hornfels and occasionally strongly pyritized. The hornfel zones are up to a few meters thick. The host schists in the inner contact aureoles were transformed into strongly pyritized andalusite–garnet–mica hornfelses, which contain higher An plagioclase and lower Fe–Mn garnet as compared to those in primary schists (Sample 1159, Table 1). The temperature during the contact metamorphism reached 600°C.

The Kvinum-1 layered massif consists of the lower ultramafic cortlandite zone (Fig. 3) and upper mafic gabbro–gabbronorite zone. The massif has a complex heterogeneous structure. Its southeastern part and the hanging wall of its central part are made up mainly of medium-grained gabbronorites and clinopyroxene–amphibole gabbros, which towards the footwall are replaced by melanocratic gabbro containing cortlandite bodies of variable thickness from tens of centimeters to 5–20 m. In the northwestern part, the massif is split into the lower and upper branches from 10–15 to 40–50 m thick, which are composed of strongly altered amphibole peridotites subsequently converting towards the hanging wall into plagioclase peridotites and amphibole gabbros. These lower and upper linear bodies contain three high-grade stringer–disseminated copper–nickel ore lodes, one of which contains a massive brecciated ore body up to 2.5 m thick [16, 20] sampled by boreholes 4 and 5 (Fig. 3).

The Kvinum-2 occurrence is located 1.2 km northwest of the Kvinum-1 occurrence (Figs. 1, 4) and consists of a 20-m-thick extended sheeted body of strongly altered cortlandites [16]. The cortlandites contain dissemination, pockets, and stringers of pyrrhotite-dominated sulfides. The highest-grade sulfide mineralization consisting of massive ores about 2.0–2.5 m thick is

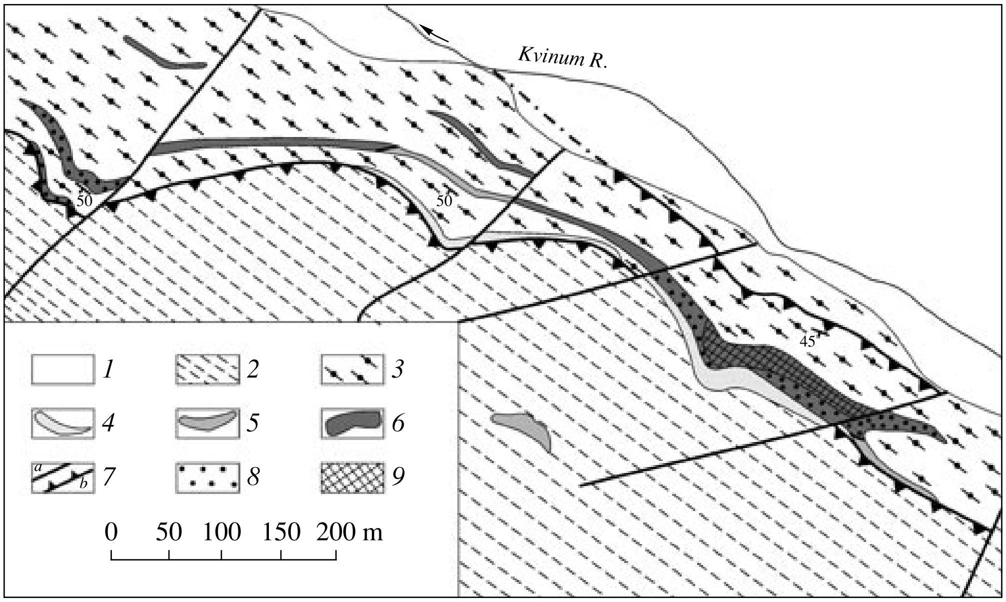

Fig. 4. Schematic geological plan of the Kvinum-2 occurrence.
(*1*) Quaternary loose deposits; (*2*) Kheivan Formation: garnet–mica ± andalusite schists, phyllites, micaceous metasandstones; (*3*) Kamchatka Group (Shikhta Formation): andalusite–garnet–mica schists: (*4*) Kola intrusive complex (?): schistose aplitic granites: (*5, 6*) Dukuk intrusive complex: gabbro, gabbronorites (*5*), cortlandites, hornblendites (*6*); (*7*) tectonic dislocations: faults (*a*), low-angle thrusts (*b*); (*8, 9*) copper–nickel ores: low-grade disseminated (*8*), high-grade massive and stringer disseminated (*9*).

located at the bottom of the cortlandite body. Upsection, the massive sulfide ores are replaced by stringer–disseminated and disseminated ores. The uppermost part of the cortlandite body almost lacks sulfide mineralization.

The Sm–Nd and Rb–Sr ages of the intrusive rocks that contain the Kvinum-1 and Kvinum-2 occurrences are within 65–67 Ma [9]. The Kuvalorogskii intrusion located southeast of the Kvinum ore field has an $^{40}Ar/^{39}Ar$ age of 57.2 ± 1.4 Ma and SHRIMP U–Pb concordia age of 50.8 ± 1.4 Ma [6]. The significant difference between the ages is related to the different formation ages of the dated minerals: amphibole and biotite represent the main phase of the emplacement, while zircon was found in the latest hybrid derivatives.

MINERALOGY OF CORTLANDITES

The amphibole peridotites (cortlandites) at the studied occurrences were deeply altered by autometasomatic processes into talc–tremolite (actinolite)–chlorite aggregate with relicts of magmatic amphibole (pargasite, tschermakite, or tschermakite hornblende) [after 23] and occasional olivine, Cr spinel, and ilmenite. The westerly Tundrovyi occurrence contains weakly altered cortlandites, whose primary mineralogy consists of olivine, pargasite, Cr-spinel, and sharply subordinate clino- and orthopyroxene (Table 3). Orthopyroxene is rarely preserved in amphibole peridotites, being almost completely replaced by cummingtonite. Small amounts of calcic plagioclase occur in the amphibole peridotites in the transition zone to the overlaying gabbroids.

Magmatic amphiboles in cortlandites are pargasite or, more often, tschermakite or tschermakite hornblende (tschermakite and tschermakite hornblende differ from pargasite in their alkali deficiency on the A site) (Table 4), which are pervasively replaced by chlorite and actinolite (Fig. 5). Such a trend in the replacement of primary amphibole is typical of both ore and barren intervals of cortlandites, being similar over the rocks and individual amphibole crystals.

Table 5 shows the average compositions of biotite, cummingtonite, Cr-spinel, and ilmenite from cortlandites of the studied occurrences. The Cr spinel exhibits an elevated Zn content. The Zn spinels are typical of sulfide copper–nickel ores and host mafic–ultramafic intrusions of many copper–nickel deposits of Central Kamchatka [19].

COPPER–NICKEL–PGE SULFIDE MINERALIZATION

Sulfide mineralization occurs in the altered cortlandites of the Kvinum ore field as lenslike bodies of massive and stringer–disseminated copper–nickel ores from 150–500 m long and from few meters to 5–20 m thick. Gabbroids of layered massifs are typically almost barren, with the exception of low-grade pyrrhotite and pyrite dissemination. The top ores were strongly oxidized and leached, thus forming a ferruginous cap. The ore bodies were studied by ditches and strippings and sampled by two boreholes (boreholes 4 and 5, Fig. 3), which recovered weakly leached stringer–disseminated

Table 3. Representative microprobe analyses of minerals from weakly altered cortlandites (sample 3776) of the Tundrovoe occurrence of the Kvinum ore field [20]

Component	Ol (n = 9)	Opx (n = 3)	Cpx (n = 3)	Hb (n = 5)	Spl (n = 14)	Pl* (n = 2)
SiO_2	39.11	52.92	49.10	40.71	0.00	57.10
TiO_2	0.00	0.21	0.83	2.88	0.44	0.00
Al_2O_3	0.00	4.79	7.28	15.79	30.56	27.92
Cr_2O_3	0.00	0.51	0.39	0.10	30.82	0.00
Fe_2O_3					6.00	
FeO	15.89	8.87	5.07	6.90	23.33	0.02
MnO	0.06	0.06	0.06	0.08	0.34	0.00
MgO	44.88	29.22	14.65	15.13	8.41	0.00
NiO	0.31	0.03	0.00	0.04	0.09	0.00
ZnO	0.00	0.00	0.00	0.00	0.32	0.00
CaO	0.06	1.38	19.76	10.49	0.00	8.79
Na_2O	0.00	0.03	0.77	3.23	0.00	6.34
K_2O	0.00	0.00	0.01	0.69	0.00	0.04
Total	100.31	98.02	97.86	96.04	100.31	100.21
X_{Mg}	0.834	0.854	0.837	0.796	0.343	–
X_{An}	–	–	–	–	–	0.433
Wo	–	2.8	44.8	–	–	–
En	–	83.1	46.2	–	–	–
Fs	–	14.1	9.0	–	–	–
Si	0.985	1.893	1.832	5.963	–	2.549
Ti	–	0.006	0.023	0.317	0.081	–
Al	–	0.202	0.320	2.729	8.830	1.470
Cr	–	0.014	0.011	0.011	5.966	–
Fe^{3+}	–	–	–	0.374	1.106	–
Fe^{2+}	0.335	0.265	0.158	0.471	4.770	0.001
Mn	0.001	0.002	0.002	0.010	0.071	–
Mg	1.685	1.557	0.814	3.302	3.068	–
Ni	0.006	0.001	–	0.004	0.018	–
Zn	–	–	–	–	0.059	–
Ca	0.002	0.053	0.790	1.646	–	0.420
Na	–	0.002	0.056	0.917	–	0.549
K	–	–	–	0.128	–	0.002

* Plagioclase occurs in cortlandites in the transition zone to the upper gabbroids. The formula units were calculated on the basis of the following: 8 (O) for Ol, 6 (O) for Cpx and Opx, 23 (O) for Hb, 32 (O) for Spl, 8 (O) for Pl. Fe^{2+} and Fe^{3+} in amphibole (pargasite) were calculated using the following formula: Fe^{3+}=Al^{IV}–Al^{VI}–2Ti–Na(A)–K(A) + Na(M_4). Fe^{2+} and Fe^{3+} in spinel were determined according to the stoichiometric formula. X_{Mg} = Mg/(Mg + Fe), X_{An} = Ca/(Ca + Na + K), and n is the number of analyses

ores in the upper part of the orebody and massive sulfide ores 2.2–2.5 m thick in its bottom.

The sulfide ores of the orebodies have a similar mineral composition, which is typical of the analogous copper–nickel deposits around the world. Massive and stringer–disseminated ores consist mainly of pyrrhotite–pentlandite–chalcopyrite assemblages (up to 90%). Less common sulfides are pyrite, sphalerite, galena, arsenopyrite, and *lollingite*, which was found for the first time in the Kamchatka ores. The apical parts of massive sulfide ores are enriched in sulfoarsenides and tellurides of Ni, tellurides and antimonides of Bi and Pd, as well as contain native gold and less common Pt arsenide and sperrylite. The central parts of the lodes are significantly lower in these minerals.

Pyrrhotite is the main ore mineral of stringer–disseminated and massive sulfide ores and occurs over the entire ore interval of the Kvinum occurrences. It occurs

Table 4. Representative microprobe analyses of relict amphibole from the Kvinum-1 and Kvinum-2 cortlandite occurrences

Component	1	2	3	4	5	6	7	8	Average (n = 8)
SiO_2	41.93	42.34	41.77	41.62	42.54	41.68	42.47	42.71	42.13
TiO_2	3.34	3.16	3.11	3.01	3.00	2.82	2.49	2.45	2.92
Al_2O_3	14.51	13.34	13.91	14.99	14.07	13.18	14.70	14.30	14.13
Cr_2O_3	0.02	0.10	0.07	0.01	0.12	0.11	0.45	0.46	0.17
FeO	12.16	10.14	10.77	12.20	9.26	9.82	9.56	9.80	10.46
MnO	0.11	0.07	0.14	0.08	0.16	–	0.09	0.08	0.10
MgO	12.03	13.07	12.20	11.50	12.51	12.91	12.93	12.53	12.46
NiO	0.03	–	0.01	0.02	0.05	–	–	–	0.03
CaO	10.62	10.82	11.01	10.94	11.15	10.50	10.93	11.00	10.87
Na_2O	1.42	1.30	1.33	1.37	1.42	2.18	1.52	1.42	1.50
K_2O	0.88	0.87	0.76	0.83	0.84	0.87	0.87	0.82	0.84
Total	97.05	95.21	95.08	96.57	95.12	94.07	96.01	95.57	95.61
X_{Mg}	0.638	0.697	0.669	0.627	0.707	0.701	0.707	0.695	0.680
based on 23 (O)									
Si	6.199	6.299	6.247	6.164	6.310	6.289	6.249	6.316	6.255
Ti	0.371	0.354	0.349	0.335	0.335	0.320	0.276	0.273	0.326
Al	2.531	2.342	2.454	2.619	2.463	2.347	2.552	2.495	2.475
Cr	0.003	0.012	0.008	0.001	0.014	0.013	0.052	0.054	0.020
Fe^{3+}	0.392	0.362	0.296	0.361	0.136	0.233	0.354	0.279	0.314
Fe^{2+}	1.112	0.899	1.051	1.150	1.012	1.006	0.822	0.933	0.012
Mn	0.013	0.009	0.018	0.010	0.020	–	0.011	0.010	0.985
Mg	2.650	2.898	2.719	2.538	2.765	2.903	2.835	2.755	2.757
Ni	0.004	–	0.001	0.003	0.006	–	–	–	0.004
Ca	1.682	1.725	1.764	1.736	1.772	1.698	1.723	1.743	1.729
Na	0.407	0.375	0.385	0.393	0.408	0.638	0.434	0.407	0.432
K	0.166	0.165	0.145	0.157	0.159	0.168	0.164	0.155	0.159

Note: the amphiboles are according to nomenclature [23]: (1, 3, 4) tschermackite, (2, 5, 7, 8) tschermackite hornblende, (6) pargasite hornblende. X_{Mg} = Mg/(Fe + Mg)

as pyrrhotite solid solution (monosulfide) and Ni-free pyrrhotite with "flamelike" pentlandite inclusions. Both varieties form aggregates from a few microns to ten or more millimeters. The mineral shows wide compositional variations: 52.7–59.9% Fe, 0–7.0 wt % Ni, and 36.7–40.2% S (Table 6) and contains minor Cu (up to 0.5%) and As (up to 3%). Pyrrhotite crystals exhibit distinct zoning expressed in the Ni decrease from the core to rim. The latest pyrrhotite generation is observed as relict inclusions in pyrite stringers and contains trace Cu (up to 0.2–0.3%). In the oxidation zone, pyrrhotite is pervasively replaced by violarite.

Chalcopyrite is second in abundance only to pyrrhotite and has a steady composition (Table 6). It crystallized slightly later than pyrrhotite and pentlandite and injects massive ores connecting with metasomatic ores that are confined to the contacts between ore bodies and host rocks. Chalcopyrite typically contains inclusions of sphalerite, galena, sulfoarsenides, and tellurides of Ni, tellurides and antimonides of Bi and Pd, and native gold.

Pentlandite is the major Ni-bearing mineral of massive and stringer–disseminated ores and occurs together with pyrrhotite and chalcopyrite. It often contains Co (up to 1%), Cu (up to 9%), and Ag (up to 12%) (Table 7) and forms separate aggregates from 1–2 μm to 10 and more millimeters in size. As pyrrhotite, pentlandite is replaced by violarite (Table 6), however, only in the oxidation zone.

Sphalerite in the form of small equant grains occurs only in chalcopyrite and contains trace Cu and Cd (Table 8).

Galena is widespread in the sulfide ores but never forms significant accumulations. As sphalerite, it forms extremely small (up to 10–20 μm) inclusions in chalcopyrite, often in association with nickel tellurides. The larger galena crystals were found only in silicate min-

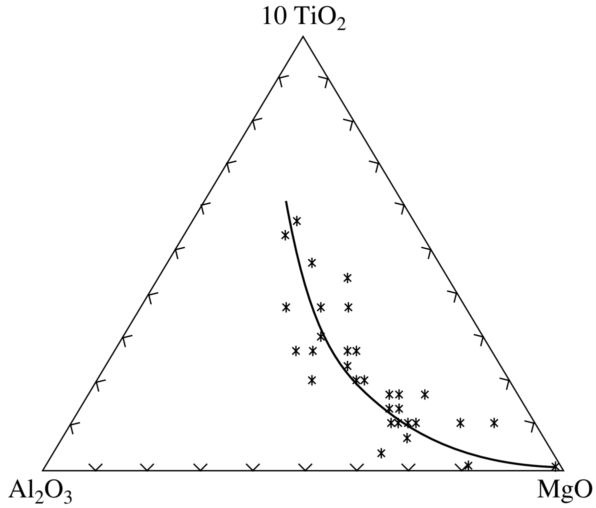

Fig. 5. Compositional trend of magmatic amphiboles in cortlandites from the Kvinum-1 and Kvinum-2 occurrences (the elements are in wt %, the total number of analyses is 150).

erals of cortlandites. Occasionally, galena contains minor bismuth (Table 8).

Besides pentlandite, Ni-bearing minerals are sulfoarsenides (gersdorffite and Co-gersdorffite containing up to 16.4% Co, as well as minerals of lollingite–safflorite–rammelsbergite series), arsenides (nickeline), and tellurides (melonite) of Ni (Table 6). *Melonite*, previously unknown in the copper–nickel ores of Kamchatka, was described here for the first time in the Kvinum-1 ores [20]. *Nickeline* has a stable composition (Table 6) with trace Sb (up to 0.22%), Te (up to 0.16%), and Co (up to 0.14%). *Gersdorffite and cogersdorffite* typically fridges nickeline or minerals of löllingite–safflorite–rammelsbergite series. All these minerals, as well as antimonides (*sudburyite*), tellurobismuthides (*michenerite*) of Pd, and *tellurobismuthite* are related to the apical parts of massive sulfide ores and to the transition zone to the stringer–disseminated ores. More rarely, they occur in the contact aureole rocks as the finest (about 10–30 μm) tabular inclusions in chalcopyrite [20].

Sperrylite (platinum arsenide) is the major Pt-bearing mineral (Table 6), being, however, strongly inferior in abundance to antimonides and tellurobismuthite of Pd, which are the major PGE-bearing minerals of the Kvinum occurrences [20].

Native gold was found in all the studied copper–nickel sulfide ores, being restricted to the areas enriched in arsenides and tellurides of Ni, Pd, and Bi. Gold forms small (5–20 μm) platelets in chalcopyrite and has a high-purity with trace Cu and Fe (Table 6). The trace Cu and Fe can be explained by the small size of the gold grains and entrapment (excitation) of Cu and Fe from host chalcopyrite during the measurements [20].

Table 5. Average compositions of cummingtonite, biotite, Cr-spinel, and ilmenite in cortlandites from the Kvinum-1 and Kvinum-2 occurrences

Component	Cummingtonite (n = 38)	Biotite (n = 6)	Cr-spinel (n = 12)	Ilmenite (n = 11)
SiO_2	56.30	38.86	–	–
TiO_2	0.05	1.22	0.52	49.39
Al_2O_3	0.18	15.67	15.30	–
Cr_2O_3	–	0.43	45.27	–
FeO	18.77	13.96	36.72	45.18
MnO	0.48	0.19	0.72	3.45
MgO	20.50	8.67	1.30	0.20
ZnO	–	–	1.28	–
CaO	0.99	–	–	–
Na_2O	0.03	0.19	–	–
K_2O	0.01	8.67	–	–
Total	97.31	94.82	101.11	98.22
X_{Mg}	0.661	0.669	–	–

Note: (n) is the number of analyses.

DISCUSSION

The copper–nickel sulfide occurrences located in the southern part of the Sredinny Range of Kamchatka, approximately 130 km northwest of Petropavlovsk–Kamchatskii are combined into the Dukuk–Kuvalorog–Kvinum ore cluster about 500 km^2 in area, which is estimated as one of the largest Kamchatka objects for sulfide PGE–Cu–Ni mineralization [3, 16, 20, 24]. The Kvinum ore field is the most promising for economic sulfide mineralization.

The stringer–disseminated and massive copper–nickel ores of the Kvinum-1 and Kvinum-2 occurrences are localized in the amphibole peridotites—the cortlandites—and form ore bodies of variable thickness from tens of centimeters to 5–20 m thick in the peridotite–gabbroid layered massifs. The massifs have a sheeted morphology and distinct layering from cortlandites at the base via plagioclase cortlandites to gabbronorites and clinopyroxene–amphibole gabbro in the roof. The massifs cut across organic-rich metasedimentary rocks of the Late Cretaceous Kheivan Formation and Kamchatka Group and, therefore, are saturated in xenoliths of the host rocks, which results in the abundance of graphite, low oxidation state of minerals, and the presence of the only oxide mineral, ilmenite.

Pyrrhotite, pentlandite, and chalcopyrite are the major ore minerals in the massive and stringer–disseminated ores with sharply subordinate pyrite, sphalerite, galena, arsenopyrite, and löllingite. Besides pentlandite, Ni-bearing minerals are also represented by sulfoarsenides (gersdorffite), arsenides (nickeline), and tellurides (melonite) of nickel [20].

The PGE mineralization is related to the upper parts of the massive sulfide ores, to the transition zone to the

Table 6. Average compositions of ore minerals from massive and stringer–disseminated occurrences in the Kvinum ore field [20]

Element	Pyrrhotite (*n* = 92)	Chalcopyrite (*n* = 53)	Pentlandite (*n* = 44)	Nickeline (*n* = 53)	Gersdorffite (*n* = 34)	Nickel sulfoarsenide (*n* = 7)	Melonite (nickel telluride) (*n* = 2)	Löllingite (*n* = 3)	Sudburyite (*n* = 3)	Michenerite (*n* = 5)	Sperrylite (*n* = 8)	Native gold (*n* = 7)	Violarite (*n* = 24)
Fe	59.14	30.40	29.13	1.04	1.54	0.39	0.35	28.21	0.47	–	–	1.84	21.99
Ni	1.83	0.14	37.38	45.20	34.22	31.12	16.83	0.31	–	0.74	–	–	31.88
Co	–	–	0.42	0.14	0.29	0.08	0.60	–	–	–	–	–	0.88
Cu	–	35.11	–	–	–	–	–	–	–	–	0.40	1.48	–
S	39.19	34.54	32.90	0.29	18.80	6.52	–	1.77	–	–	0.37	–	39.96
As	–	–	–	55.02	45.49	63.44	–	71.83	–	–	42.97	–	–
Sb	–	–	–	0.22	0.24	–	0.29	–	52.03	1.65	–	–	–
Bi	–	–	–	–	–	–	–	–	1.18	44.89	–	–	–
Te	–	–	–	0.16	0.13	–	82.24	–	0.78	27.55	–	–	–
Pd	–	–	–	–	–	–	–	–	44.76	22.68	–	–	–
Pt	–	–	–	–	–	–	–	–	–	–	54.27	–	–
Ag	–	–	–	–	–	–	–	–	–	–	–	12.55	–
Au	–	–	–	–	–	–	–	–	–	–	–	85.52	–
Total	100.16	100.19	99.83	101.55	100.71	101.55	100.31	102.12	99.22	97.50	98.01	101.40	99.70

Note: (*n*) is the number of analyses. Nickel sulfoarsenide belongs to the minerals of the safflorite–rammelsbergite series. Violarite is the secondary mineral replacing pyrrhotite, pentlandite, and, to a lesser extent, chalcopyrite.

Table 7. Representative microprobe analyses of cobalt-, copper-, and silver-bearing pentlandite from the orebodies of the Kvinum ore field

Element	Cobalt-bearing pentlandite				Copper-bearing pentlandite		Silver-bearing pentlandite			
Fe	26.22	27.04	28.95	28.37	28.35	28.71	32.22	34.10	33.12	33.39
Ni	39.44	38.39	36.89	36.08	31.06	27.04	20.42	20.82	20.67	21.60
S	32.68	33.00	32.46	32.77	33.11	33.55	31.85	31.81	31.72	31.35
Co	0.91	0.93	1.10	1.30	0.41	0.35	–	–	–	–
Cu	–	–	–	–	6.34	9.50	2.21	0.80	1.56	0.23
Ag	–	–	–	–	–	–	12.09	11.84	12.00	12.38
Total	99.25	99.35	99.40	98.52	99.27	99.15	99.79	99.37	99.07	98.95

Table 8. Representative microprobe analyses of sphalerite and galena from sulfide ores of the Kvinum occurrences.

Element	Sphalerite					Galena		
	1	2	3	4	5	6	7	8
Fe	6.75	8.60	8.53	8.60	8.77	1.42	0.30	0.51
S	33.91	33.18	32.29	33.33	33.20	12.76	12.42	13.12
Zn	59.82	52.99	54.14	53.54	51.41	–	–	–
Cu	0.94	1.96	1.00	1.83	2.21	–	–	–
Cd	–	2.88	2.99	3.20	3.53	–	–	–
Pb	–	–	–	–	–	84.83	82.43	85.83
Bi	–	–	–	–	–	–	3.58	–
Total	101.42	99.61	98.95	100.50	99.12	99.01	98.73	99.46

stringer–disseminated ores, and, more rarely, to the contact aureole rocks. The same intervals of ore bodies are enriched in arsenides and tellurides of Ni, Pd, and Bi, and contain high-purity native gold. The central parts have insignificant PGE and Au contents. PGE mineralization includes predominant antimonides (sudburyite) and tellurobismuthides (michenerite) of Pd, with sharply subordinate platinum arsenide (sperrylite).

It is suggested that the contents of major sulfide minerals and the productivity of PGE mineralization in the cortlandites is defined by complex processes of magmatic differentiation and sulfurization of ultramafic derivatives under the effect of fluids, which are accumulated at the crystallization front of the massifs and cause layering of mafic–ultramafic magmas with strong separation of sulfur between them [10, 11]. The fluid-assisted layering of the mafic–ultramafic massifs resulted in contrasting separation of PGM as a reflection of the uneven sulfur distribution between melts. Chromite-bearing ultramafic complexes of ophiolites usually host Ir–Ru–Os mineralization, which is subsequently replaced by Pt and Pd mineralization in the massifs of mafic complexes [10]. Such a change in the PGE mineralization corresponds to subsequent increasing of the chemical affinity for sulfur (as well as As and other elements) in accordance with their distribution coefficients between sulfide and basic melts. The productivity of PGE mineralization significantly increases with increasing content of S, As, Te, and Bi, to which Pt and, especially, Pd exhibit high chemical affinity, in fluids causing liquid immiscibility.

Since the studied layered massifs of the Kvinum ore field were solidified from bottom to top, the highest grade PGE mineralization is localized in the upper parts of cortlandite-contained massive ores and in the transition zone to the stringer–disseminated ores, as that in the Merensky Reef of the Bushveld Massif [8, 10].

CONCLUSIONS

Detailed data on the geology and mineralogy of the host metamorphic rocks, the mineralogy of sulfide ores, and the distribution of PGE mineralization were obtained for the Kvinum-1 and Kvinum-2 copper–nickel occurrences of the Kvinum ore field, the most promising targets for copper–nickel–PGE mineralization in the Sredinny Range of Kamchatka.

It was established that the stringer–disseminated and massive copper–nickel ores are associated with amphibole peridotites (cortlandites) and form ore bodies varying in thickness from a few tens centimeters to 5–20 m in the layered cortlandite–gabbroid massifs of the Late Cretaceous Dukuk intrusive complex. Massive sulfide ores were found only at the bottom of the cortlandite bodies and grade upward into the stringer–disseminated and disseminated ores.

It was shown that the ore bodies are made up mainly of pyrrhotite, chalcopyrite, and pentlandite, with sharply subordinate pyrite, sphalerite, galena, arsenopyrite, and löllingite. Besides pentlandite, Ni-bearing minerals include sulforasenides (gersdorffite), arsenides (nickeline), and tellurides (melonite) of nickel.

It was found that PGE mineralization is dominated by antimonides (sudburyite) and tellurobismuthides (michenerite) of Pd with sharply subordinate platinum arsenide (sperrylite) and occurs in the apical parts of the massive sulfide zones and in the transition zone to the stringer–disseminated ores. Ore intervals enriched in arsenides and tellurides of Ni, Pd, and Bi contain high-purity gold. The central parts of the orebodies are low in PGE and native gold.

It is suggested that the contents of major sulfide minerals and the productivity of PGE mineralization in the cortlandites are defined by combined differentiation and sulfurization of ultramafic derivatives under the effect of fluids, which were accumulated at the crystallization front and caused layering of parental magmas with sulfur separation [10, 11]. The fluid-assisted layering of mafic–ultramafic massifs resulted in a contrasting distribution of PGM as a response to an uneven distribution of sulfur (as well as As, Te, and Bi) during immiscible splitting. The productivity of PGE mineralization significantly increases when fluid causing liquid immiscibility becomes higher in S, As, Te, and Bi, to which Pt and, especially, Pd reveal high chemical affinity.

ACKNOWLEDGMENTS

We are grateful to V.I. Sidorenko our colleague of the (Territorial Agency on the Interior Use of the Kamchatka Oblast and Koryak Autonomous Okrug) for help in studying the geology of the copper–nickel occurrences of the Kvinum ore cluster of Kamchatka.

Rewiewer A.A. Marakushev

REFERENCES

1. O. V. Avchenko, *Mineral Equilibria in Metamorphic Rocks and Geobarometry* (Nauka, Moscow, 1990) [in Russian].
2. L. L. Perchuk, I. V. Lavrent'eva, L. Ya. Aranovich, and K. K. Podlesskii, *Biotite–Garnet–Cordierite Equilibria and Evolution of Metamorphism* (Nauka, Moscow, 1983) [in Russian].
3. N. A. Goryachev, S. M. Rodionov, V. V. Ratkin, et al., "Metallogenic Belts and Ore Regions in Eastern Russia," in *The Kvinum Metallogenic Belt. Geodynamic, Magmatism, and Metallogeny in Eastern Russia*, Ed. by A. I. Khanchuk (Dal'nauka, Vladivostok, 2006) [in Russian].
4. S. S. Zimin, *Formation of Nickel-Bearing Hornblende Mafic Rocks in the Far East* (Nauka, Novosibirsk, 1973) [in Russian].
5. *Map of Mineral Resources of Kamchatka. Scale 1:500 000*, Ed. by A. F. Litvinov, M. G. Patoka, B. A. Markovskii, et al. (Vseross. Geol. Inst., St. Petersburg, 1999) [in Russian].

6. E. G. Konnikov, V. M. Chubarov, A. V. Travin, et al., "Formation Time of the Ni-Bearing Norite-Cortlandite Association of East Asia," Geokhimiya **44** (5), 564–570 (2006) [Geochem. Int. **44** (5), 516–521 (2006)].
7. I. V. Lavrent'eva and L. L. Perchuk, "Phase Equilibrium in Biotite–Garnet System: Experimental Data," Dokl. Akad. Nauk SSSR **260** (3), 731–734 (1981).
8. V. G. Lazarenkov, S. V. Petrov, and I. V. Talovina, *Platinum Group Metal Deposits* (Nedra, St. Petersburg, 2002) [in Russian].
9. E. A. Landa, B. A. Markovskii, B. V. Belyatskii, et al., "Age and Isotopic Signatures of Alpine-Type, Zonal, and Layered Mafic–Ultramafic Complexes of Kamchatka," Dokl. Akad. Nauk **385** (6), 812–815 (2002) [Dokl. Earth Sci. **385A** (6), 727–729 (2002)].
10. A. A. Marakushev, "Origin of Platinum Group Metal Deposits and Their Experimental Modeling," in *Platinum of Russia*, Ed. by V. P. Orlov (ZAO "Geoinformmark," Moscow, 1995), Vol. II, pp. 49–63 [in Russian].
11. A. A. Marakushev, N. A. Paneyakh, I. A. Zotov, et al., "The Jinchuan Copper–Nickel Deposit in China and the Relation of the PGE Mineralization to the Ultrabasic Rocks Alkalinity," Geol. Rudn. Mestorozhd. **42** (5), 440–458 (2000) [Geol. Ore Deposits **42** (5), 397–413 (2000)].
12. M. A. Mishkin, *Metamorphism in Asian Continent–Pacific Ocean Transition Zone System* (Nauka, Moscow, 1981) [in Russian].
13. V. M. Okrugin, V. A. Poletaev, and V. M. Chubarov, "The Shanucha Ore Field," in *Geodynamics, Magmatism, and Metallic Mineralization in Eastern Russia*, Ed. by A. I. Khanchuk (Dal'nauka, Vladivostok, 2006), Book 2, pp. 575–576 [in Russian].
14. L. L. Perchuk, *Rock Forming Mineral Equilibria* (Nauka, Moscow, 1970) [in Russian].
15. L. P. Plyusnina, *Experimental Studies of Mafic Metamorphism* (Nauka, Moscow, 1983) [in Russian].
16. V. A. Poletaev, "Platinum–Copper–Nickel Sulfide Deposits and Occurrences of Peridotite–Pyroxenite–Norite Formation of Central Kamchatka," in *Platinum of Russia*, Ed. by V. P. Orlov. (ZAO "Geoinformmark," Moscow, 1999), Vol. III, Book 1, pp. 191–199 [in Russian].
17. V. A. Poletaev, "Geological–Economic Estimation of Inferred Multicomponent Copper–Nickel Sulfide Deposits in Central Kamchtka," Ed. by V. I. Goncharov, in *Proceedings of the All-Russian Conference on Geodynamics, Magmatism, and Mineralogy of the Continental Margin of the Northern Pacific Ocean, Magadan, Russian, 2003* (Sev. Vost. Kompl. Nauch.-Issled. Inst. Daal'nevost. Otd. Ross. Akad. Nauk, Magadan, 2003), Vol. 3, pp. 187–188 [in Russian].
18. A. V. Solov'ev, Doctoral Dissertation in Geology and Mineralogy (Moscow, 2005).
19. V. M. Chubarov, "Zn Spinels from Nickel-Bearing Mafic Intrusions of Central Kamchatka," in *New Data on the Petrology of Magmatic and Metamorphic Rocks of Kamchatka*, Ed. by Yu. A. Martynov (Dal'nevost. Otd. Akad. Nauk SSSR, Vladivostok, 1989), pp. 157–167 [in Russian].
20. V. M. Chubarov, E. K. Ignat'ev, S. V. Moskaleva, et al., "The Kvinum-1 Copper–Nickel Prospect in Cortlandites, the Southern Sredinnyi Range, Kamchatka," Dokl. Akad. Nauk **403** (2), 231–236 (2005) [Dokl. Earth Sci. **403**, 710–714 (2005)].
21. S. A. Shcheka and V. M. Chubarov, "Nickel-Bearing Cortlandtites of Kamchatka," Izv. Akad. Nauk SSSR, Ser. Geol., No. 12, 50–61 (1987).
22. S. A. Shcheka and A. A. Vrzhosek, "PGE Mineralization of Mafic–Ultramafic Assemblages in the Far East of Russia," in *Platinum of Russia*, Ed. by V. P. Orlov (ZAO "Geoinformmark," Moscow, 1999), Vol. III, Book I, pp. 66–75 [in Russian].
23. B. E. Leake, "Nomenclature of Amphiboles," Can. Mineral. **16** (4), 501–520 (1978).
24. W. J. Nokleberg, R. J. Miller, V. V. Naumova, et al., "Project on Mineral Resources, Metallogenesis, and Tectonics of Northeast Asia," US Geol. Surv. Open-File Rept. 03-203 (2003). Internet Address: http://geopubs.wr.usgs.gov/ open-file/of03-203.
25. E. K. Ravna, "Distribution of Fe^{2+} and Mg between Coexisting Garnet and Hornblende in Synthetic and Natural Systems: An Empirical Calibration of the Garnet-Hornblende Fe–Mg Geothermometer," Lithos **53** (3–4), 265–277 (2000).